

Graphitization in High Carbon Commercial Steels

M.A. Neri, R. Colás, and S. Valtierra

(Submitted 21 February 1997; in revised form 5 January 1998)

Graphitization kinetics in two commercial high carbon steels, AISI types 1075 and 1095, are studied by conducting a series of isothermal annealing treatments in the temperature range of 560 to 680° C for periods of time ranging from 20 to 500 h. The samples selected were collected along the processing route in a commercial production line dedicated to the fabrication of thin strip. The structures studied were those of hot rolling (consisting of fine pearlite), cold rolling (spheroidized carbides within a deformed ferritic matrix), and subcritical annealing (spheroidized carbides in undeformed ferrite). The samples obtained from hot rolled coils do not graphitize, whereas those cold rolled graphitize at a rate that depends on the type of steel and degree of deformation. No graphite was found in samples from the lower carbon steel, which were subcritically annealed, although they were observed in specimens from the other steel, which were cold rolled to a reduction of 50% prior to the subcritical annealing.

Keywords annealing, deformation, graphitization, high-carbon steels, kinetics

1. Introduction

Study of the solid state transformation in commercial steels rely on the metastable iron-cementite (Fe_3C) diagram, rather than on the stable iron-graphite diagram (Ref 1, 2) because the decomposition of austenite into ferrite and either cementite or graphite requires the enrichment of carbon on the parent phase as it is expelled from ferrite, and formation of carbide will be favored over graphite mainly due to its higher solubility in ferrite (Ref 2).

Decomposition of cementite into iron and graphite may occur when steels are annealed or treated for long times above room temperatures (Ref 3-12). The transformation rate seems to depend on the microstructure of the material. For instance, some authors (Ref 3-11) find that quenched and tempered steels graphitize faster than when they are normalized (Ref 9-11). There is also experimental evidence (Ref 4) that this transformation occurs at a higher rate in coarse structures, obtained after conducting a full annealing, than in the finer structures which result from normalizing. Results reported elsewhere (Ref 6) point in the same direction because full annealing of hot rolled steel previous to cold rolling has been found to accelerate the transformation, although another author (Ref 6) reports higher graphitization rates in samples of normalized rather than in annealed steel. The amount of deformation imparted to the samples prior to the treatment appears to have a very strong effect in graphitization (Ref 5, 8, 9, 12), even greater than that of quenching and tempering (Ref 8).

Chemical composition of the material seems to be another factor affecting the rate of decomposition. Trials conducted in

steels of different carbon content demonstrate that this phenomenon appears at an earlier stage in materials with higher content in this element (Ref 4, 8, 13). There is experimental evidence that elements like silicon, nickel, and aluminum, which exhibit a tendency to concentrate in ferrite (Ref 13-15), accelerate this transformation (Ref 8-14).

The results of a study conducted on samples of steels of two different nominal compositions, which were treated at different temperatures and times, is presented here to evaluate the possibility of reducing the temperature at which the subcritical annealing is conducted in a steel factory.

2. Experimental Procedure

Samples were collected in a factory, which cold rolls thin strip high carbon steel. Special care was taken to obtain samples of the material before and after the intermediate subcritical annealing treatments programmed to facilitate the rolling process. The thicknesses and reductions imparted in the different samples of the two steels studied (namely AISI 1075 and 1095) are presented in Table 1; specimens cut from the initial hot-

Table 1 Samples obtained for the present study

Specimen	Steel	Thickness, mm	Reduction, %	Structure
A.1	1075	1.90	0.0	Mixture of ferrite and pearlite
A.2	1075	1.27	33.0	Spheroidized carbides in ferrite
A.3	1075	0.60	53.0	Spheroidized carbides in ferrite
B.1	1095	1.90	0.0	Mixture of ferrite and pearlite
B.2	1095	0.64	50.0	Spheroidized carbides in ferrite
B.3	1095	0.36	44.0	Spheroidized carbides in ferrite
B.4	1095	0.20	43.0	Spheroidized carbides in ferrite
B.5	1095	0.14	32.5	Spheroidized carbides in ferrite

M.A. Neri, Centro de Investigación en Materiales Avanzados, Leon Tolstoi 166, Complejo Industrial Chihuahua, 31109 Chihuahua, Chih., México; R. Colás, Facultad de Ingeniería Mecánica y Eléctrica, Universidad Autónoma de Nuevo León, A.P. 149-F, 66451 Cd. Universitaria, N.L., México; S. Valtierra, Corporativo Nemark, S.A. de C.V., A.P. A-100, 64000 Monterrey, N.L., México.

rolled band are identified as A.1 and B.1. Figure 1 shows schematically the rolling schedule (performed out with four-high and cluster mills) employed to manufacture the strip as well as the places within the processing route at which the subcritical treatments are programmed (referred to as either batch or subcritical annealing in this work).

One of the problems encountered when gathering the samples was the difficulty of cutting them from the same coil, or at

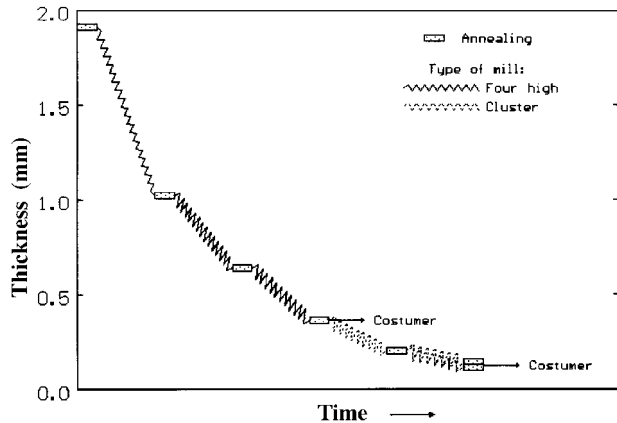


Fig. 1 Schematic diagram of the reduction schedule showing the types of rolling mills employed and the annealing treatments given to the strips

least the same shipment of coils, which would be translated in the study of a single chemical composition. Much effort was used to ensure that at least samples of equal thickness (cold rolled and batch annealed) came from the same coil. Chemical compositions of the different samples are presented in Table 2.

Graphitization in the specimens cut from the samples obtained while at the industrial plant was promoted by means of isothermal annealings. These treatments were conducted from

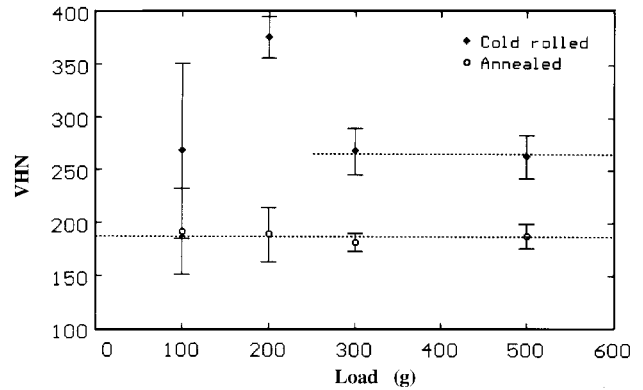
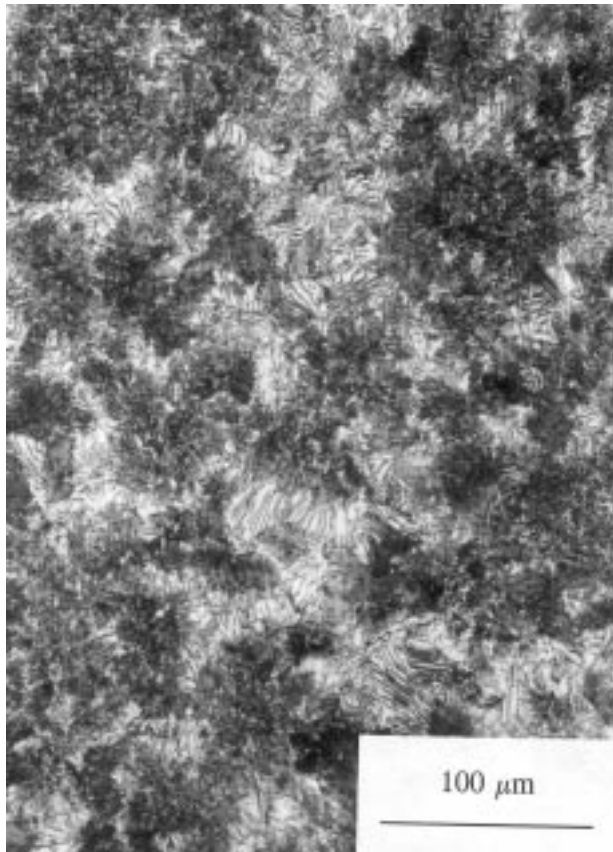
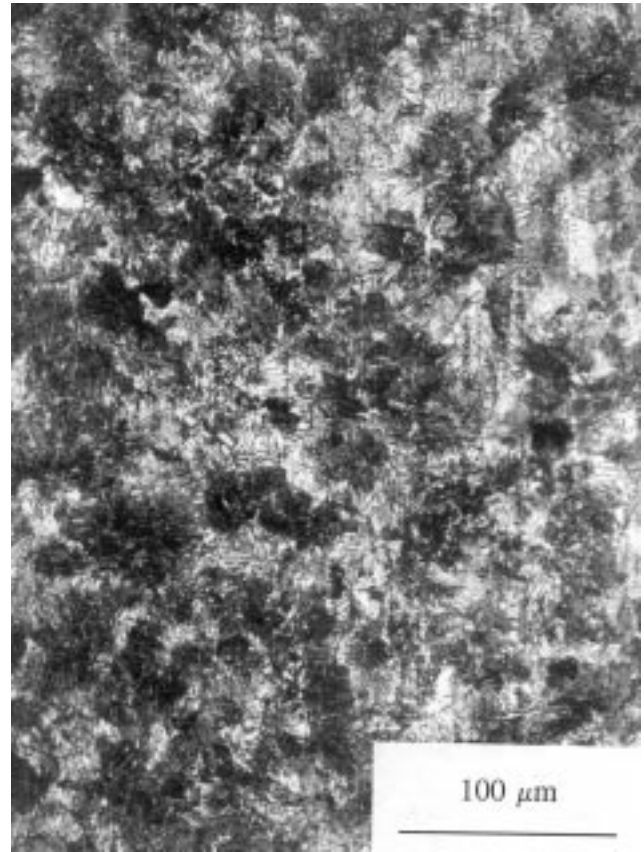


Fig. 2 Hardness variation as a result of varying loads. Tests were performed in cold-rolled and annealed samples of AISI type 1095 steel 0.64 mm in thickness (B.2).



(a)



(b)

Fig. 3 Microstructures of the hot-rolled AISI type (a) 1075 and (b) 1095 steels

the 560 to 680° C temperature range for periods of times ranging from 20 to 500 h. The specimens were immersed in neutral salt baths, 70% BaCl₂, 30% NaCl, rectified every 8 h with small amounts of NH₄Cl (Ref 16) to avoid oxidation. The interval of temperatures was selected to study the possibility of decreasing the temperatures at which the subcritical annealings are conducted in plant, which is approximately 710° C.

Graphitization kinetics were studied by image analysis on metallographic sections of the specimens subjected to the isothermal treatments. The parameters recorded were number of graphite nodules per unit area, fraction of area covered by the

nodules, highest equivalent, and mean diameter of the nodules. The metallographic observations were performed at 200×, but the area of the specimen observed varied as a function of strip thickness. For instance, the area analyzed in each observation on the thicker samples (1.27 mm) was of 178,000 μm², whereas that on the thinner ones (0.137 mm) was of 33,030 μm². Analysis of variance indicated that the difference in area observed was of no statistical significance. Results from each of the observed areas analyzed were averaged, and the 95% confidence limit was obtained after assuming that the measurements followed a normal distribution, in which case the upper limit is

Table 2 Chemical analysis of the samples

Sample	Steel	Composition, wt%									
		C	Mn	P	S	Cu	Ni	Si	Cr	Al	N (ppm)
A.1	1075	0.75	0.61	0.014	0.001	0.03	0.02	0.22	0.17	0.026	140
A.2	1075	0.70	0.59	0.020	0.001	0.07	0.03	0.22	0.10	0.044	67
A.3	1075	0.73	0.66	0.020	0.001	0.07	0.06	0.21	0.17	0.045	189
B.1	1095	1.03	0.41	0.017	0.003	0.02	0.02	0.17	0.20	0.000	124
B.2	1095	0.96	0.42	0.015	0.001	0.09	0.06	0.19	0.17	0.022	68
B.3	1095	0.96	0.42	0.015	0.001	0.09	0.06	0.19	0.17	0.022	68
B.4	1095	0.96	0.43	0.019	0.001	0.11	0.07	0.17	0.17	0.020	171
B.5	1095	1.01	0.39	0.021	0.001	0.10	0.07	0.21	0.18	0.000	132

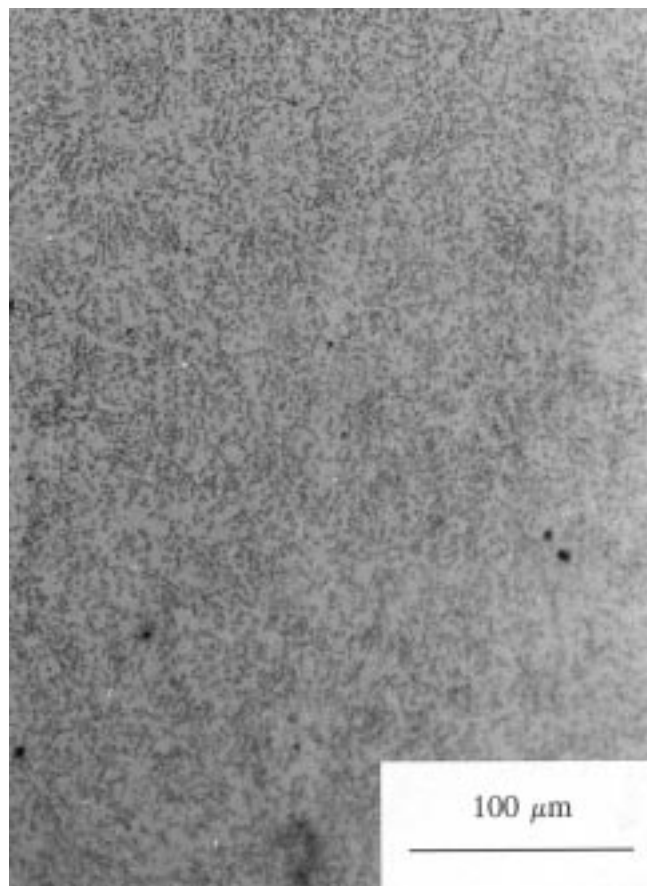


Fig. 4 Microstructure of the cold-rolled AISI type 1075 steel to a thickness of 1.27 mm (A.2)

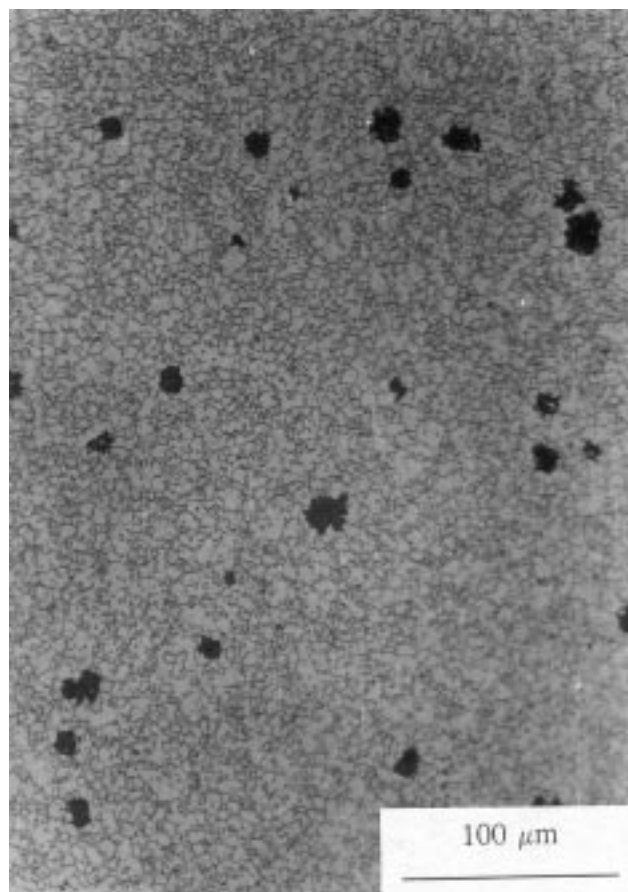


Fig. 5 Graphite nodules (black) observed after annealing for 100 h at 650 °C a sample of the cold-rolled AISI type 1095 steel of 0.64 mm in thickness (B.2)

equal to the average value plus two times the standard deviation, while the lower one is obtained by subtracting twice the standard deviation from the average value.

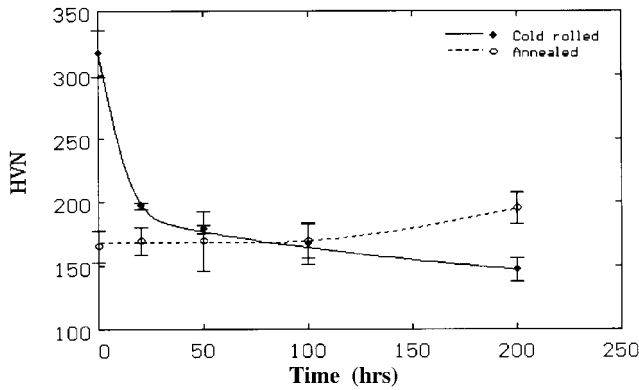


Fig. 6 Microhardness variation as a function of the isothermal annealing time for cold-rolled and batch annealed samples of the AISI type 1095 steel 0.64 mm in thickness (B.2)

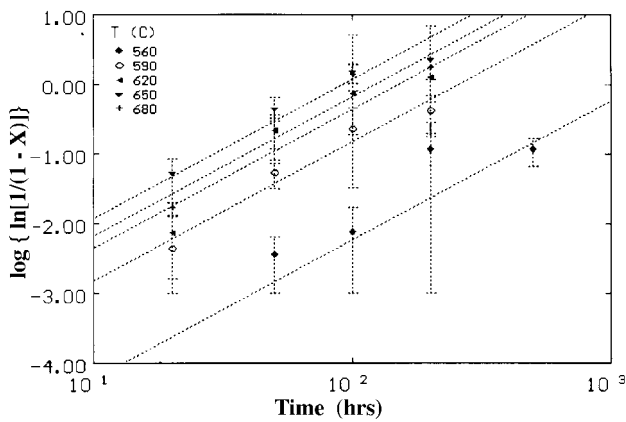


Fig. 7 Series of lines passed through the 95% confidence limits of the experimental measurements conducted on samples of the AISI type 1095 steel of 0.64 mm in thickness (B.2)

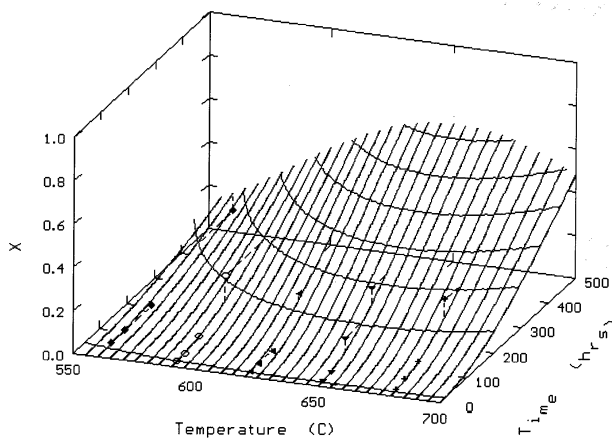


Fig. 8 Graphitization in the cold-rolled AISI type 1075 steel of 1.27 mm in thickness (A.2)

The transformed fraction, X , of iron carbide into graphite was calculated on stoichiometric basis, assuming that the end of decomposition, $X = 1$, will be achieved when all the carbide transforms into graphite. Vickers microhardness tests were conducted on deformed and annealed samples. A load of 300 g was selected after finding that this one is the lowest one, which will provide consistent and reproducible results. See Fig. 2.

3. Results

Microstructures of the samples cut from the original material, (A.1 and B.1 in Tables 1 and 2) are presented in Fig. 3. The fine pearlite appreciated in them is the result of hot rolling and air cooling. The aim of the intermediate batch annealings between passes is to reduce the strength of the material. The subcritical annealings are normally conducted at temperatures of approximately 710 °C to promote the spheroidization of cementite. A typical batch annealing cycle is approximately 80 h, of which 20 to 30 h are for soaking. Figure 4 shows the typical microstructure for the 1.27 mm thick sample of the AISI type 1075 steel (specimen A.2). No systematic variation of the ferritic grain resulting from the subcritical anneal was observed, independent of the type of steel or reduction. The average measured values in all the samples ranged from 10 to 14 μm .

Not all the samples subjected to the isothermal annealings showed the transformation of cementite into graphite and ferrite. This phenomenon was not observed in either of the hot-rolled specimens, nor in the annealed samples of the AISI type 1075 steel. Graphitization was only observed in some of the specimens from the AISI type 1095 steel (B.2 and B.5), although the decomposed amount was limited to a small fraction.

The behavior observed in the cold-rolled samples was different because the presence of graphite nodules was observed in almost all cases. The only exception was the 0.60 mm thick strip of the AISI type 1075 steel (A.3). An example of the graphite nodules is shown in Fig. 5 where the microstructure of a deformed 0.64 mm thick (B.2) specimen of the AISI type 1095 steel is shown.

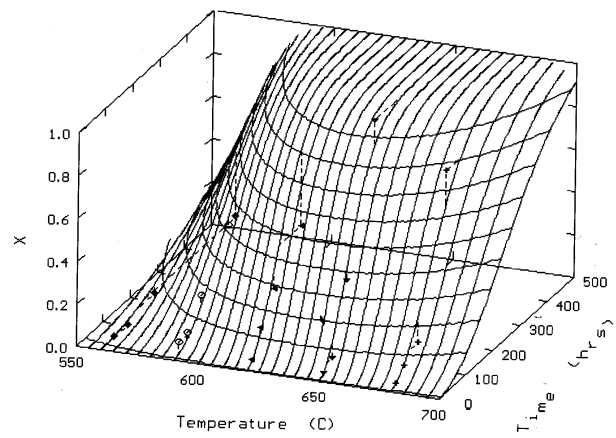


Fig. 9 Graphitization in the cold-rolled AISI type 1095 steel of 0.14 mm in thickness (B.5)

The microhardness varied depending on whether the isothermally treated samples were cold rolled or were subjected to the subcritical annealing treatment. The typical behavior is

shown in Fig. 6 for the case of the AISI type 1095 steel of 0.64 mm thickness (2.2). In this figure, the strong softening effect occurs at the beginning of the treatment in the cold-rolled

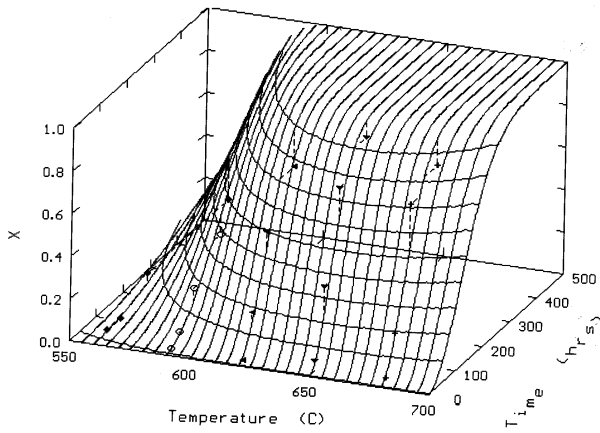


Fig. 10 Graphitization in the cold-rolled AISI type 1095 steel of 0.64 mm in thickness (B.2)

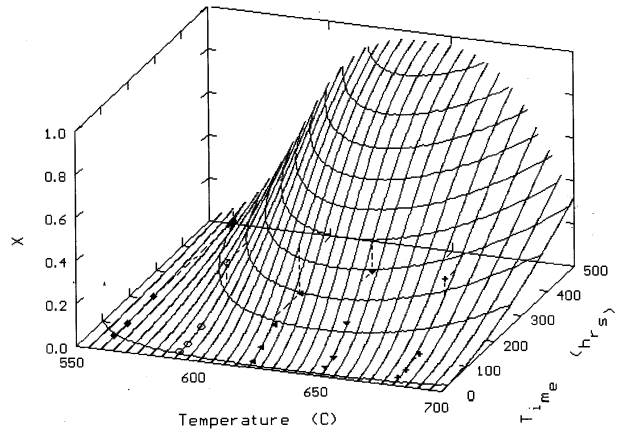


Fig. 11 Graphitization in the subcritically annealed AISI type 1095 steel of 1.27 mm in thickness (B.2)

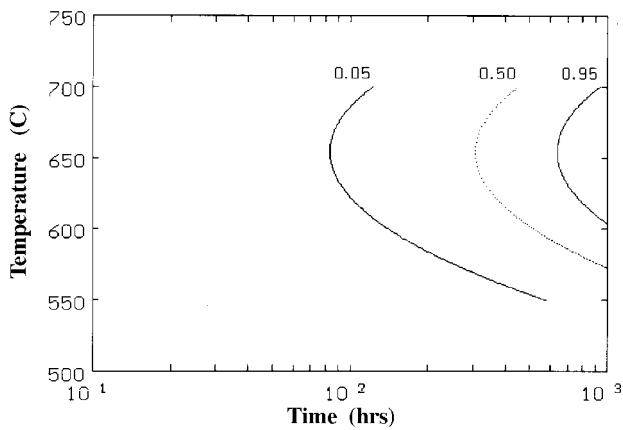


Fig. 12 Isothermal transformation diagram for the cold-rolled AISI type 1075 steel of 1.27 mm in thickness (A.2)

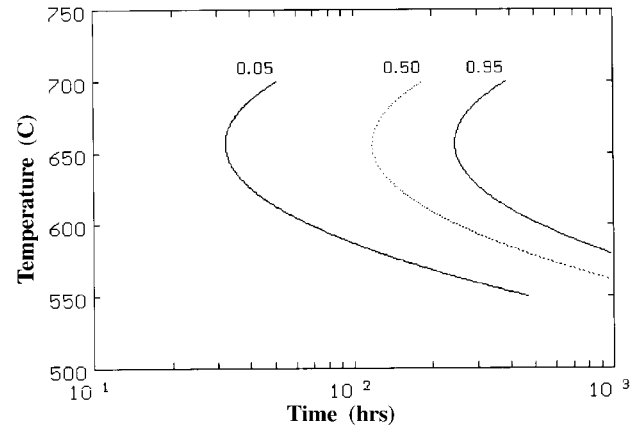


Fig. 13 Isothermal transformation diagram for the cold-rolled AISI type 1095 steel of 0.14 mm in thickness (B.5)

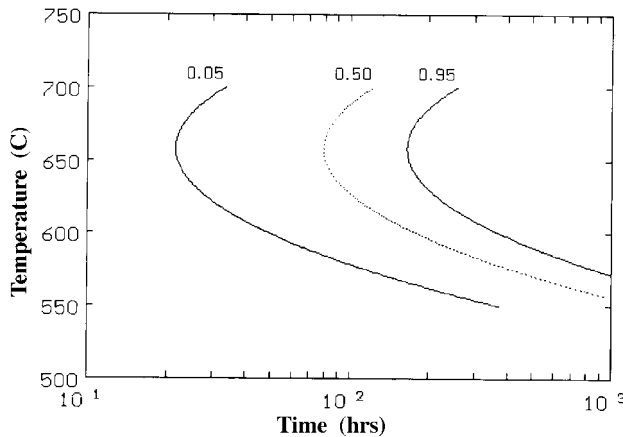


Fig. 14 Isothermal transformation diagram for the cold-rolled AISI type 1095 steel of 0.64 mm in thickness (B.2)

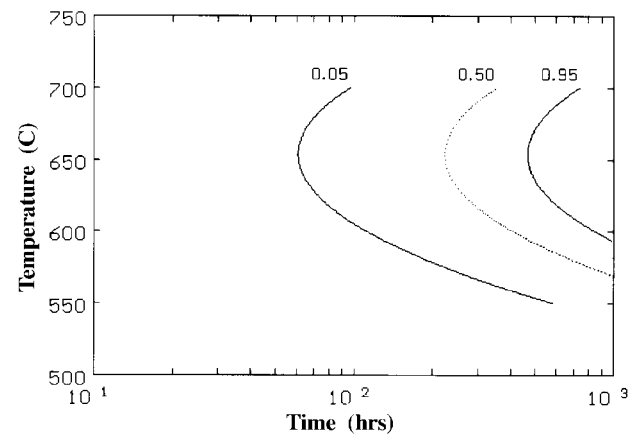


Fig. 15 Isothermal transformation diagram for the subcritically annealed AISI type 1095 steel of 1.27 mm in thickness (B.2)

samples, which can be attributed to the occurrence of restoration (Ref 17), whereas the hardness remains independent of time in the batch annealed samples. It can also be observed that the hardness after the isothermal treatment on cold-rolled samples is lower than the hardness measured in the subcritically annealed samples.

4. Discussion

Analysis of the transformed fraction, X , of cementite into ferrite and graphite was performed once the information relative to its progress was available. Data of this fraction were adjusted to kinetic equations of the type:

$$X = 1 - \exp(-kt^n) \quad (\text{Eq 1})$$

where t is the time, k is a temperature dependent coefficient, and n is the reaction exponent, which varies from 1.5 to 2.5 when growth is controlled by diffusion (Ref 18). It was not possible to determine the systematic variation of n and k with temperature due to the high dispersion of the experimental data, and it was decided to set n equal to two, following earlier results in which growth of the nodules was attributed to carbon diffusion (Ref 8).

The values of k were found by passing a series of lines through the 95% confidence limit of the experimental determination on the transformed fraction at the different times of the isothermal tests. An example is presented in Fig. 7 for the case of the cold-rolled 0.64 mm thick strip of the AISI type 1095 steel. The values of k were then fit to a second degree polynomial to evaluate its temperature dependence.

Figures 8 and 9 show the evolution of the transformed fraction in the two types of steels deformed to a reduction of approximately 33% (samples A.2 and B.5). In them it is possible to observe the marked increase in rate of transformation as the carbon content augments. Another feature associated with the higher carbon steel was the occurrence of decomposition in some of the samples, which were subcritically annealed prior to the isothermal tests, a phenomenon which was not observed to occur in the AISI type 1075 steel. In these figures, the experimental measurements are identified by the same symbols employed in Fig. 7, whereas the full lines correspond to the behavior predicted by fitting the values of k to second degree polynomials.

Figures 10 and 11 show the behavior observed in the samples reduced to the greatest extent (50%, samples B.2) in the AISI type 1095 steel before and after the subcritical annealing conducted in the factory. These results indicate that either the in-plant treatment was not efficient enough to eliminate the distortion on the material, or that the strain was high enough to promote the formation of graphite nuclei during the subcritical annealing (conducted in the factory), which were then able to grow during the isothermal experiments.

From the plots shown in Fig. 8 to 11, it was possible to construct a series of isothermal transformation diagrams (Fig. 12 to 15), in which the conditions (time and temperature) required to achieve a transformed fraction of 0.05, 0.50, and 0.95 are drawn. All of these diagrams indicate that the fastest rate of

transformation occurs from approximately 650 to 660 °C, which agrees with results from previous researchers (Ref 6, 13, 14). In this way, it was possible to appreciate how the decomposition of the steels increase with the amount of carbon (Fig. 12 and 13) and with the increment of deformation (Fig. 13 to 14). For instance, it can be appreciated that the increase of carbon from approximately 0.75 to 0.95 translates in the reduction of the time to start transformation (considered to be at $X = 0.05$) from 84 to 32 h when the steel has given a 33% reduction in height (Fig. 12 and 13). When the deformation in the higher carbon steel is increased to a reduction of height of 50%, this time is reduced to 22 h (Fig. 14).

This work was to study the possibility of reducing the annealing temperature, a fact which might not be feasible when the AISI type 1095 steel is subjected to reductions of approximately 50%, because it is clear from Fig. 14 that this phenomenon might take approximately 25 h to occur (which is not a long time for a spheroidizing treatment) with annealing at temperatures of approximately 680 °C. The only way in which the subcritical annealing temperature can be reduced without exposing the steel for graphitization is by reducing at the same time the amount of carbon in the steel.

5. Conclusions

Results from this work indicate that graphite nodules form at the temperature interval of 650 to 680 °C, a feature which eliminates the possibility of reducing the temperature normally employed during spheroidizing treatment.

The most favorable microstructure for the decomposition of cementite into ferrite and graphite is that resulting from cold rolling. This transformation was observed during the isothermal treatment of samples cut from the higher carbon steel and subjected to subcritical annealings in the factory, but since these particular specimens were reduced in height by more than 50%, it is not possible to eliminate the possibility that the start of transformation occurred during the spheroidization treatment, rather than during the isothermal ones.

Acknowledgments

The authors acknowledge the support given by CONACYT and the facilities provided by Cintacero, S.A. de C.V.

References

1. H. Okamoto, *Phase Diagrams of Binary Iron Alloys*, ASM International, 1992
2. L.S. Darken and R.V. Gurry, *Physical Chemistry of Metals*, McGraw Hill Publishing Co., 1953
3. C.R. Austin and M.C. Fetzlar, *Trans. ASM*, Vol 35, (No. 485), American Society for Metals, 1945
4. M.A. Hughes and J.G. Cutton, *Trans. ASM*, Vol 37, (No. 110), American Society for Metals, 1946
5. J.H. Andrew and H. Lee, *J. Iron Steel Inst.*, Vol 165, (No. 145), 1950
6. B.F. Brown, *Brit. Weld. J.*, Vol 72, (No. 889), 1954
7. G.V. Smith and B.W. Royle, *Trans. ASM*, Vol 48, (No. 320), 1955
8. A. Rosen and A. Taub, *Acta Metall.*, Vol 10, (No. 501), 1962
9. H. Sueyoshi and K. Suenaga, *Rev. S. Jap. Metaux*, Vol 42, (No. 676) 1978

10. L.E. Samuels, *Optical Microscopy of Carbon Steels*, American Society for Metals, 1980
11. F. Ternon, *Sv. Techn. Aerosp. Rep.*, Vol 23, (No. 21), 1983
12. V.I. Bidash and A.I. Prikhod'ko, *Met. Sci. Heat Treat.*, Vol 29, (No. 116), 1987
13. G.T. Higgins and G.V. Jeminson, *J. Iron Steel Inst.*, Vol 203, (No. 146), 1965
14. J.E. Harris, J.A. Whiteman, and A.G. Quarrel, *Trans. AIME*, Vol 233, (No. 168), 1965
15. W.C. Leslie, *Physical Metallurgy of Steel*, McGraw Hill, 1980
16. B.E. Becherer, Vol 4, *Heat Treating, ASM Handbook*, ASM International, 1991, p 726
17. R.W. Cahn, *Physical Metallurgy*, 3rd ed., R.W. Cahn and P. Haasen, Ed., North-Holland Physics Publishers, 1983, p 1595
18. J.W. Christian, *The Theory of Phase Transformations in Metals and Alloys*, 2nd ed., Pergamon Press, 1975